Electronic Supplementary Material (ESI) for Photochemical & Photobiological Sciences.

Supporting Information to

Photoelectrocatalytic Degradation of Emerging Contaminants at $WO_3/BiVO_4$ Photoanodes in Aqueous Solution.

Vito Cristino[a], Luisa Pasti[a]*, Nicola Marchetti[a], Serena Berardi[a], Carlo Alberto Bignozzi[a] Alessandra Molinari[a], Francesco Passabi[a], Stefano Caramori*[a], Lucia Amidani[b], Michele Orlandi,[c] Nicola Bazzanella,[c] Alberto Piccioni[d], Jagadesh Kopula Kesavan[d], Federico Boscherini[d] and Luca Pasquini[d]

(a) Department of Chemical and Pharmaceutical Sciences, University of Ferrara, Via L. Borsari 46, 44121 Ferrara, Italy.

(b) Helmholtz-Zentrum dresden-Rossendorf, c/o European Synchrotron Radiation Facility, 71 Avenue des Martyrs, 38000 Grenoble, France.

(c) Physics Department of the Trento University, Via Sommarive 14, 38123, Povo, Trento, Italy

(d) Department of Physics and Astronomy, University of Bologna, Viale C. Berti Pichat 6/2, 40127, Bologna, Italy.

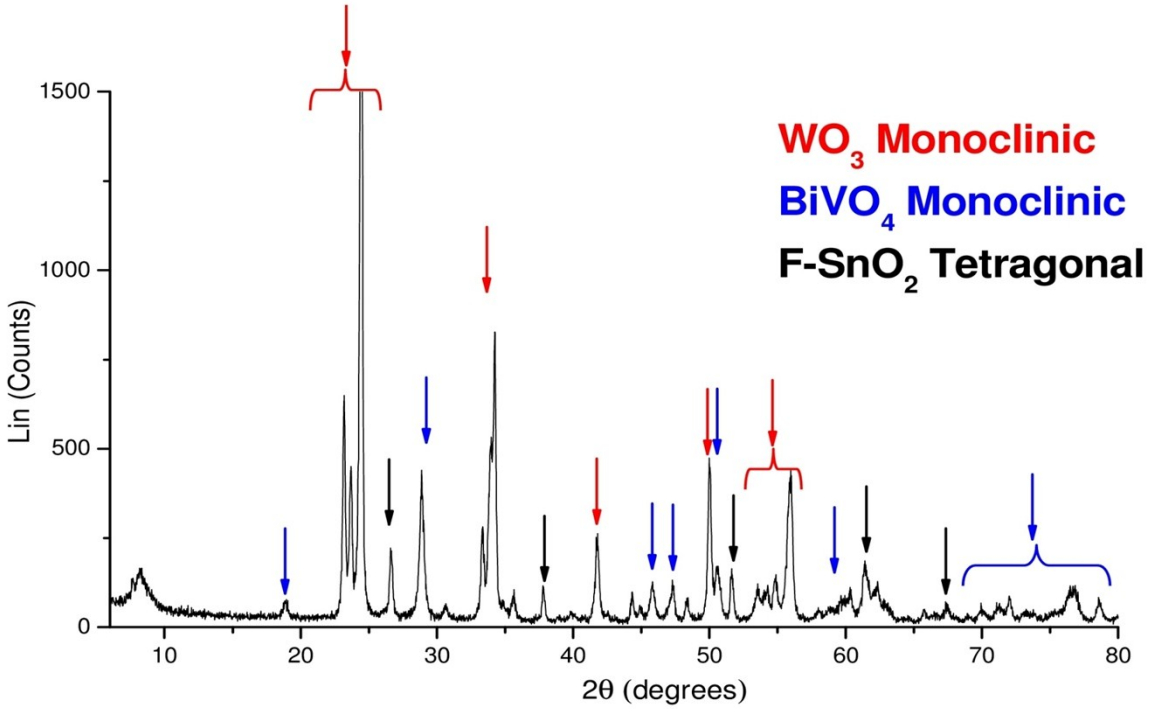

Figure S1. X ray diffractogram confirming the monoclinic crystal structure of $BiVO_4$ (blue arrows). Diffraction peaks assigned to WO_3 (red arrows) and to the underlying ohmic support (Fluorine doped Tin Oxide, black arrows) are also well evident. No V (V) oxide was detected within the sensitivity of this technique.

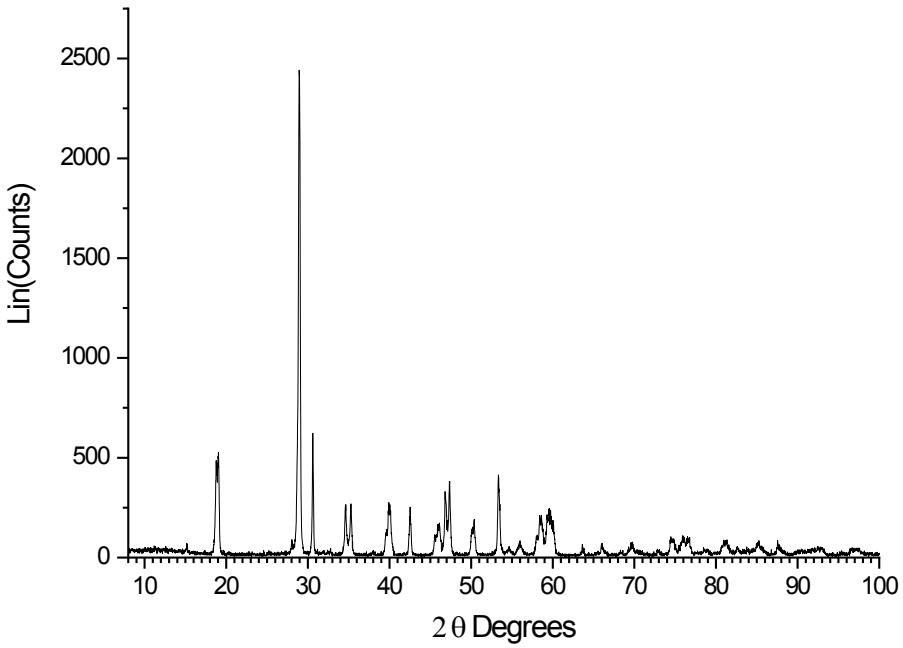

Figure S2. XRD of $BiVO_4$ powder

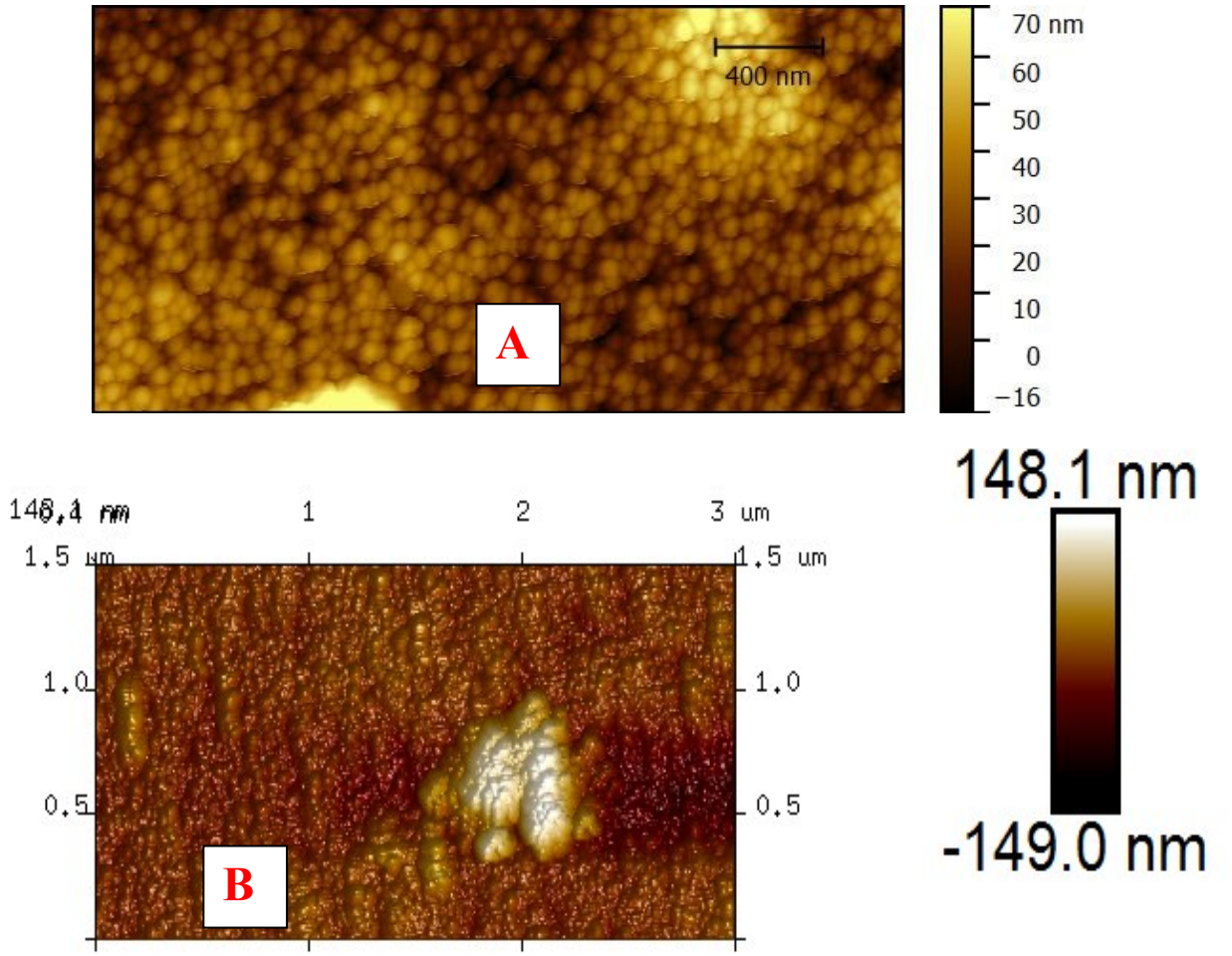

Figure S3. Wide area (3x3 µm) AFM imaging of WO_3 (A) and $WO_3/BiVO_4$ (B) thin films. In (A) the presence of relatively large and monodisperse particles is evident compared to (B), where a smoother appearance is due to the presence of smaller particles, covering and filling the voids between the WO_3 ones.

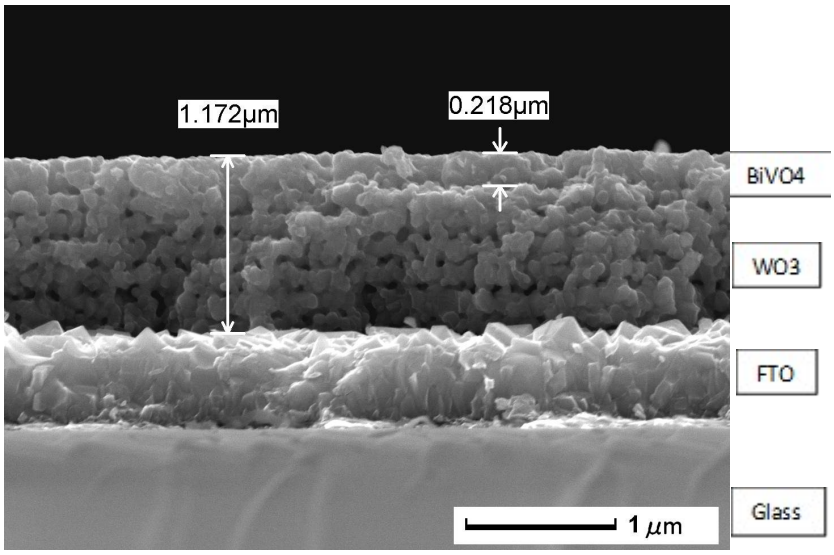
1.172µm
0.218µm
BiVO4
WO3
FTO
Glass
1 µm

(A)

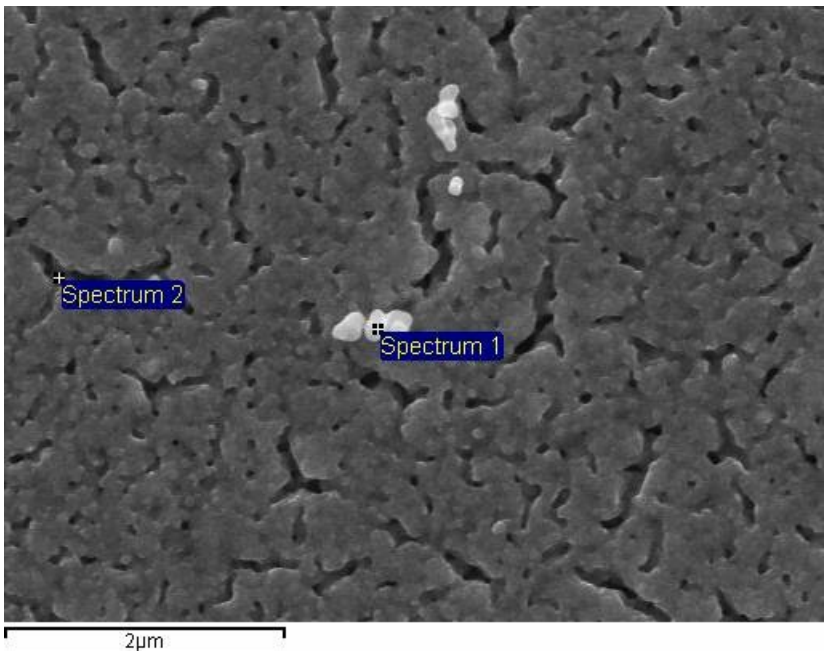
Spectrum 2
Spectrum 1
2µm

(B)

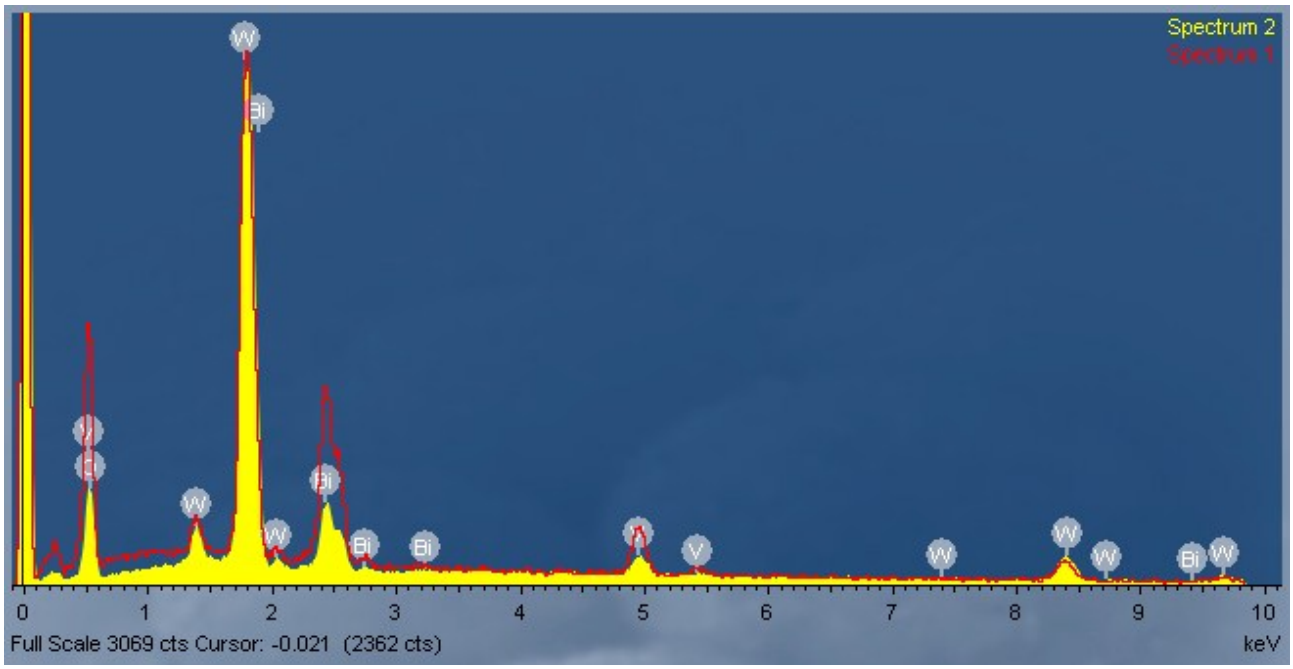

(C)

Figure S4: (A) Cross sectional view of the $WO_3/BiVO_4$ heterojunction; (B) Thin film surface with spots sampled by EDS analysis (C) showing the elemental contributions of Bi, W and O as the only significant constituents of the interface.

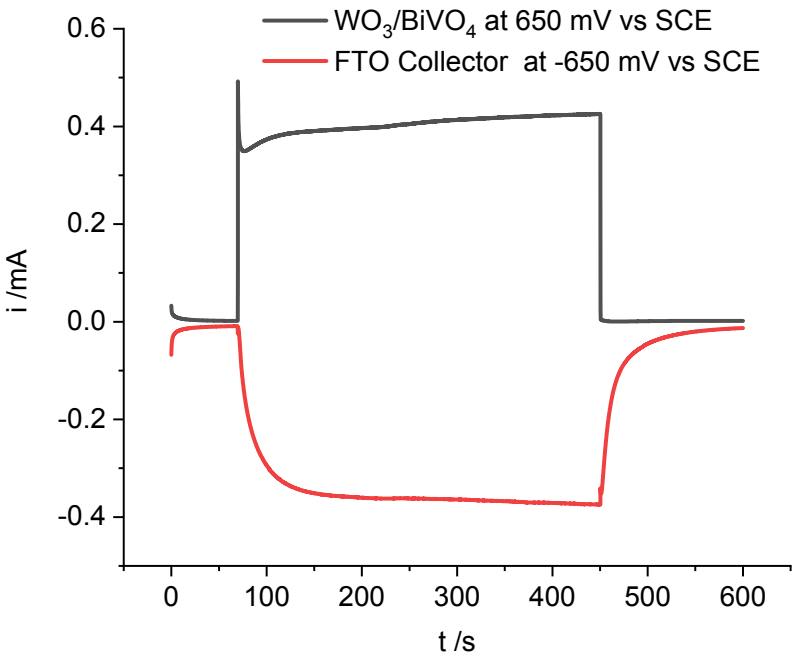

Figure S5. Generator/Collector experiments in oxygen detection with $WO_3/BiVO_4$ biased at 0.65 V vs SCE under AM 1.5 G illumination. 0.5 M Na_2SO_4 at pH 7.

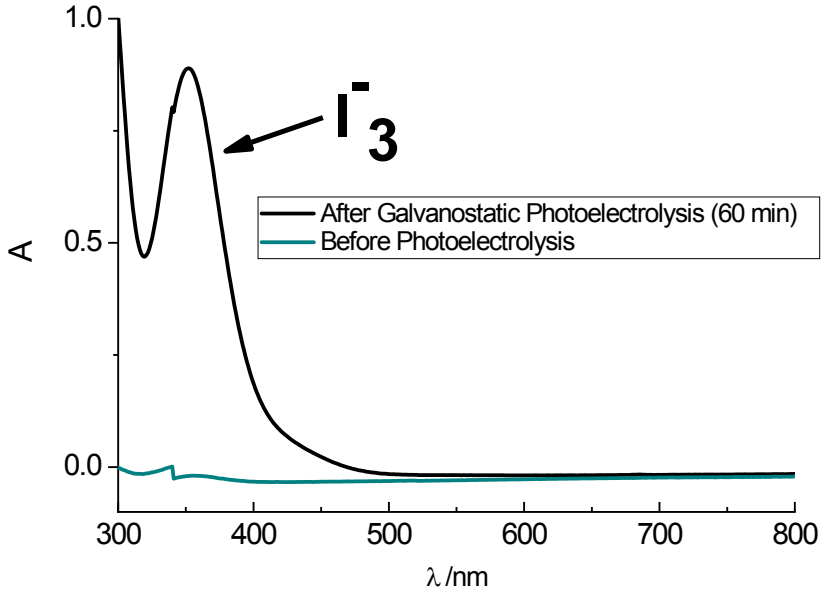

Figure S6. Detection of H_2O_2 through I_3^- formation following addition of excess NaI to photoelectrolyzed 0.5 M Na_2SO_4.

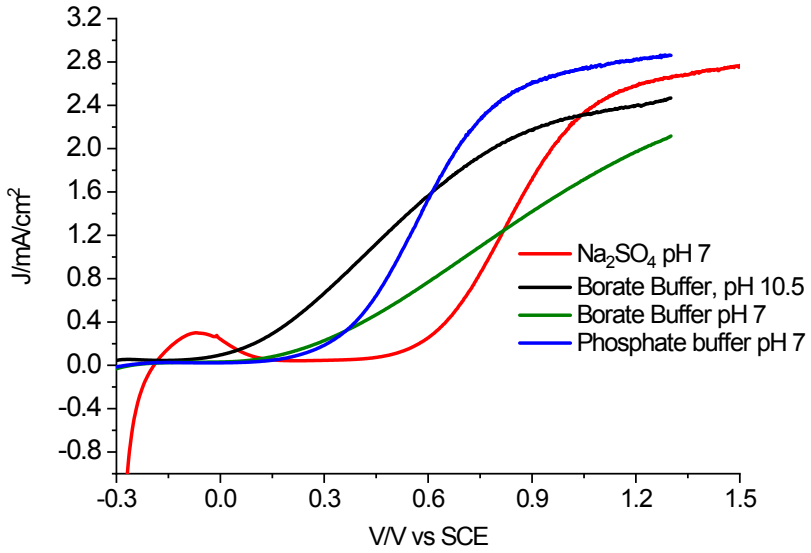

Figure S7. J/V curves in phosphate and borate buffers compared to Na_2SO_4. The electrolyte concentration was 0.5 M in all cases.

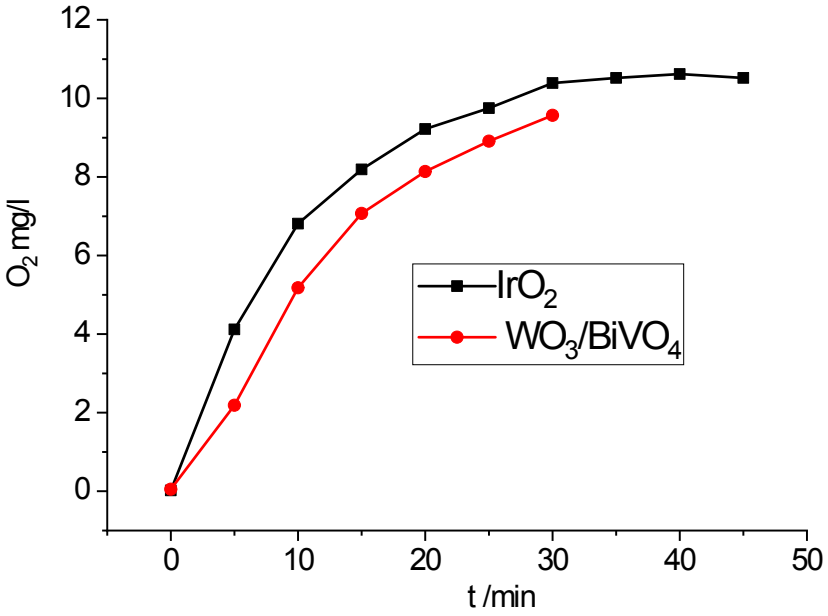

Figure S8. Oxygen evolution in phosphate buffer determined during constant potential electrolysis. At the same voltage (0.65 V vs SCE) at which in the Na_2SO_4 electrolytes 0.5 mA/cm^2 are obtained, here ca. 2 mA/cm^2 are observed, consistent with the JV curves of Figure S6. Saturation of the solution with dissolved oxygen thus occurs within the first 30 minutes of photoelectrolysis. Reference IrO_2 is here galvanostatically biased at a current of 2mA/cm^2

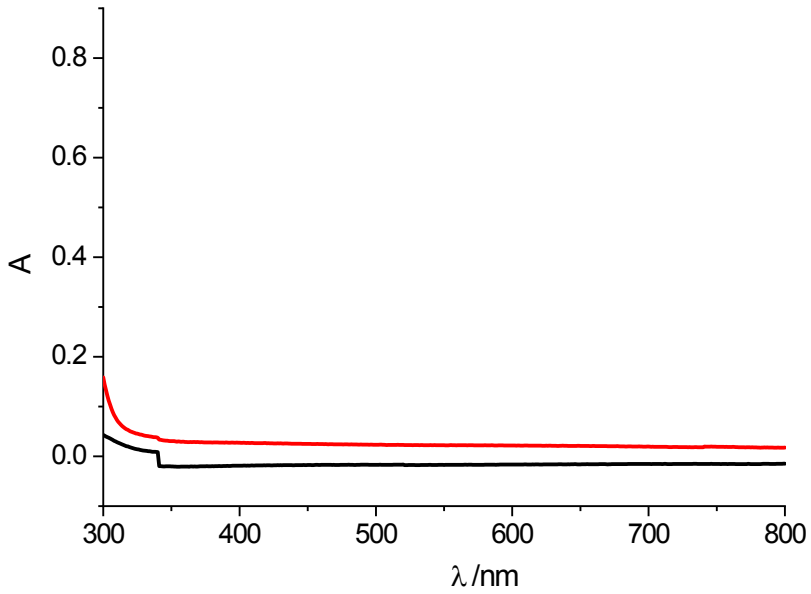

Figure S9. Detection of H_2O_2 through I_3^- formation following addition of excess NaI to photoelectrolyzed 0.5 M phosphate buffer. The peak centred at 356 nm, evident in Figure S5 was absent in this case.

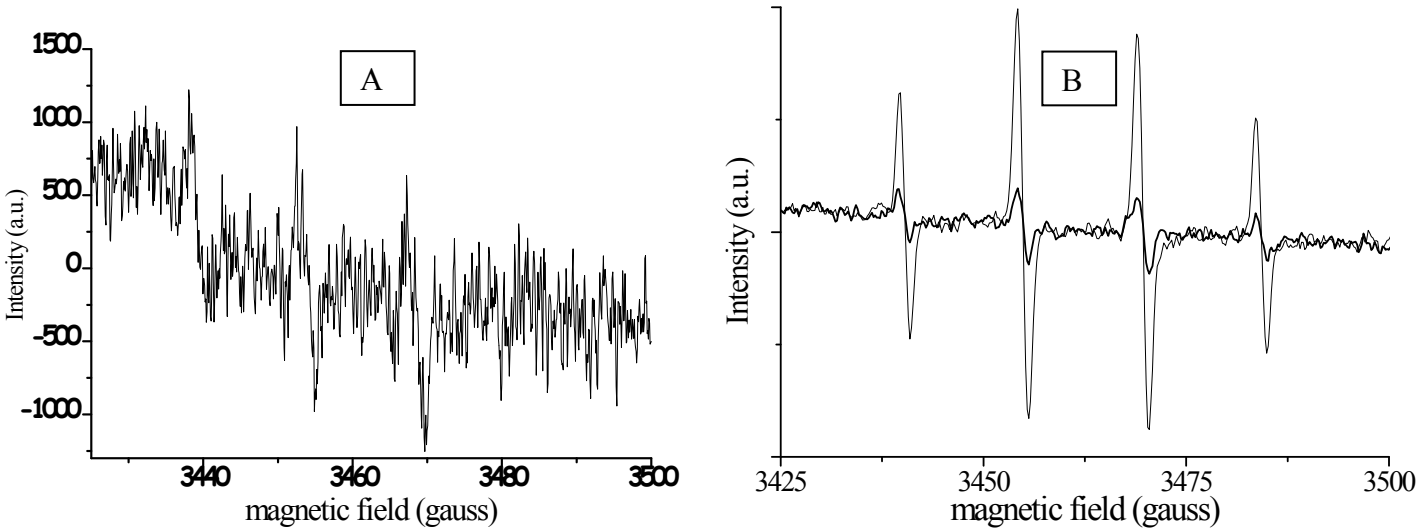

Figure S10. ESR spectra of $BiVO_4$ (A) and WO_3 (B) suspensions in water during $\lambda > 420$ nm illumination in the presence of DMPO as a spin trap. The very weak signal in Figure 3 A is a triplet, probably resulting from the coupling with N in a decomposition of DMPO produced under illumination.

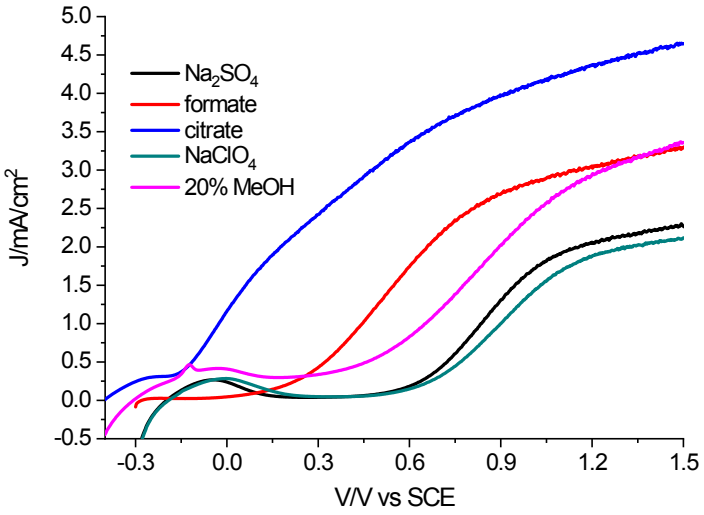

Figure S11. J/V curves of $WO_3/BiVO_4$ under front AM 1.5 G illumination in the presence of different organic hole scavengers at pH 7. The concentration of the sodium salts was always 0.5 M. Methanol was present in 20% V/V in sodium sulphate.

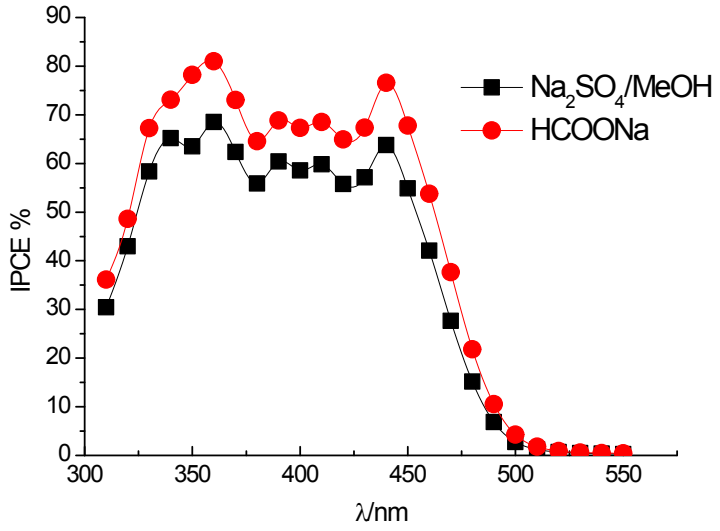

Figure S12. IPCE spectra (front illumination mode) recorded in the presence of sacrificial agents at neutral pH at 1.2 V vs SCE. Upon excitation of the semiconductor $IPCE = \varphi_{e/h}\varphi_{tr}\varphi_{if}$, ($\varphi_{e/h}$, φ_{tr} and φ_{if} are the quantum yield of charge generation, charge transport, and interfacial charge injection respectively); $\varphi_{e/h} = 1$ (every absorbed photon results in the creation of an electron/hole pair) and if $\varphi_{if} \approx 1$ in the presence of good hole scavengers, it follows that the maximum IPCE is essentially determined by the efficiency of charge transport across the interpenetrated junction.